DEPARTMENT OF PHYSICS

University of Strathclyde Science

**PH450 Report 2021-22**

# Evaluating Spot Finding Methods

**Submitted in partial fulfilment for the degree of MPhys**

Anton Gashi
Registration No.: 201914462

*SUPA Department of Physics, University of Strathclyde, Glasgow G4 0NG, United Kingdom*

Dr Sebastian van de Linde (Primary Supervisor) and Dr Daniel Oi, (Secondary Supervisor)
(Dated: 4th April 2022)

# Abstract

Sub-pixel localisation and spot finding are methods employed in several different areas of research like microscopy, small form factor satellites and in some cases LIDAR (Light Detection and Ranging). During this project a new method for spot finding was developed and tested against industry standard techniques in order to improve accuracy whilst also reduce computational time, this task is in the context of algorithms that need to be resource efficient but have improved accuracy compared to previous methods. The method proposed is similar to a Gaussian fitting method but with less computational complexity. This method tries to fit a triangle function overtop a spot of light that follows a point spread function in order to find the centre of that spot of light. This new method, compared to centroiding, was unfortunately marginally less accurate in most applications and much slower also, however it does show some promise in places where centroiding usually fails like in high noise situations and where box size limitations are a factor. This method shows potential and steps should be carried out in order to further the accuracy.

# Acknowledgements

Firstly I would like to thank both my supervisors Dr Sebastian van de Linde and Dr Daniel Oi, they were both great at helping, guiding and supporting me through this project. I would also like to thank my friends and family who were always there to be relied on if and when needed.

# Contents

# List of Figures

# I. Introduction

## A. Sub-Pixel Localisation

Super-resolution microscopy is the process of taking the diffraction limit of a microscope, 250nm in the x and y direction, and improving it at a minimum by a factor of 2 although more modern methods improve it by up to a factor of 10. In the past this has been achieved by ensemble techniques like SIM (Structured Illumination Microscopy) and STED (Stimulated Emission Depletion). SIM takes advantage of the moiré effect which is an interference pattern created by two similar grated patterns that overlap, this produces an apparent pattern. In the case of SIM the patterns are the unknown sample structure emission of the desired object that is being imaged, and the other is a specifically constructed excitation light intensity. These moiré patterns observed can also be much coarser than the grated patterns and may be easily observable in the microscope. [1] An improvement on these methods is single-molecule microscopy, in which molecules are individually fluoresced and imaged instead of ensembles which helps distinguish more detail and produce better results than the diffraction limit. There are two ways that this general method have been implemented; photo-activated localisation microscopy(PALM) and stochastic optical reconstruction microscopy(STORM), both rely on fluorophores which are fluorescent chemicals that re-emit light after being excited. This helps as the fluorescence emits the light stochastically so only a subset of molecules "light-up" at once, this is important as if they are separated by at least 200nm then they can be located to nanometre precision. Since the molecules are now separated spatially this process needs to just needs to be repeated until all molecules have been "switched-on", this gives a stack of images with blurry spots which can be located and recombined into a final image with spot-precision on the order of $<$ 20nm.[2] The resolution of a super-resolution image usually doesn't refer to the spot-precision of the located molecule, rather it refers to the structural resolution, this can be calculated along with the density of fluorophores as the Nyquist-Shannon sampling theorem states a minimum number of fluorophores are required to resolve the structure (equation 2). [3][4]

### *1. Pixels and Resolution*

In the Modern Dictionary of Electronics by Graf a pixel is described as a, spatial resolution element. The smallest distinguishable and resolvable area in an image. [5] This was mainly in reference to an analog image but the principle applies to a raster image, which is a $N \cdot M$ matrix of values that display colour and intensity. In the specific case of the spot localisation that the Methods section (II) describe the images are $N \cdot N$ and 16-bit black and white.

Resolution is the capability of resolving two points or lines. Since super-resolution by definition changes the resolution of the input images, the resolution of the output image needs to be quantified. Firstly the uncertainty of a spatial measurement is set by the equation;

$$\sigma_{x,y} \sim \frac{\sigma_{PSF}}{\sqrt{N}} \tag{1}$$

Where $\sigma_{PSF}$ is the standard deviation of the point spread function (PSF) for the microscope, and $N$ is the number of detected photons per florescent event. Since the relationship of equation 1 is approximately the inverse square root, the more detected photons the lower the uncertainty becomes.[6] One of the ways to calculate the maximum resolution achievable is by using the Nyquist-Shannon sampling theorem, this states that any detail in a measurement that is smaller than twice the size of the average label to label distance can not reliably be resolved.[7] The Nyquist resolution limit can be written formally as;

$$\text{Nyquist resolution limit } = \frac{2}{N^{\frac{1}{D}}} \tag{2}$$

Where $N$ is the density of labels, and $D$ is the dimensionality. Labels in this specific case refers to each individual fluorescent event that is detected by the camera, the density of labels is sometimes constrained by the molecules being detected as if the structure that's trying to be detected is too sparse the uncertainty remains relatively high. For example if the resolution was desired to be 20nm in one dimension then fluorophores have to be separated at least 10nm apart at a density of $10^4 \mu m^{-2}$ at a minimum to achieve it. The final resulting uncertainty of any image is therefor the maximum of either equation (1) or (2).

### *2. Fluorophores*

Single molecule super-resolution demands the switching of fluorophores stochastically, this can be done reversibly or irreversibly. Reversible switching fluorophores are photo-activated and emit light until it becomes non-fluorescent again unless reactivated. Irreversible switching fluorophores either start in the off state or the on state, if it starts in an off state it can be photo-activated and turned on then after a period of time it becomes bleached. If it starts switched on then it can be further excited and transition to a red-shifted state.[3]

According to equation 2 the resolution is increased if the number density $N$ is increased, although in order to locate or find a spot in a diffraction limited image the spots need to be spaced apart. Therefor the rate at which populations are on or off can be denoted by $k_{on}$ and $k_{off}$, also the rate at which the fluorophores switch to the on and off states matter and are denoted as $\tau_{on}$ and $\tau_{off}$. The switch rates are directly linked with how many excitations can be detected at once and thus are linked with the ability to accurately find the location of each spot. Ratios between on and off states are denoted as $r = \frac{k_{off}}{k_{on}} = \frac{\tau_{off}}{\tau_{on}}$, the larger the ratio, r, the more accurate results can be up until a point.

## B. Motivation

The main motivation behind my project is to improve the accuracy of spot finding methods whilst keeping the computational time to a minimum. That is to say this project should be aiming to produce a method of spot-finding that either less complex, less computations per localisation, fewer steps or a mixture of all. This method will be tested against centroiding, an algorithm known for obtaining good results quickly. Additionally another motivation is to create a method that is particularly resistant to background noise.

The applications of spot finding reach far beyond localisation microscopy it can be used in other technologies, for example a paper published by Castorena and Creusere [8] has the problem of needing a fast super-resolution technique to get higher spatial resolution from their LIDAR (Light Detection and Ranging) system. This system is constrained by the laser spot size and precision of the scanning mechanical unit as the single laser source with sampling rates in the GHz range which achieves high accuracy for depth and range resolution but poor spatial resolution. A consideration was to decrease the diameter of the laser thus increasing the spatial sampling density, although this was deemed too computationally expensive.

With the almost exponentially increasing launching of small form factor satellites such as the CubeSat, arises the challenge of efficiently utilising the satellites computing resources. This means any segment of code being ran on the satellite needs to run as quickly as possible whilst keeping a certain standard of accuracy, especially for the processes that the satellite depends on to operate like attitude control, power management and calculations for orbital maneuvers. The main method used for orienting(attitude control) CubSat like satellites is by using a Star Tracker, this works by using a camera mounted facing stars that are known to the satellite via a star catalogue and moves based on how aligned or unaligned a reference image is with the actual image seen.[9] The method

in which the image is processed so it can be compared to the reference is called spot finding, this entails taking the image and finding each bright spot or star accurately. The motivation for this project is to develop a spot finding method for star tracking and compare it to the state of the art algorithms measuring accuracy, precision and speed.

# II. Methods

## A. Centroiding

The most common way of spot finding for star tracking is to use centroiding algorithms, this is when a subsection of pixels are considered to be a star using a rough calculation. The area of interest is then filtered in such a way that reduces noise and aberrations, finally apply the algorithm in this case it's the centre of gravity method (3)(or the moment method)[10][11].

$$(x_b, y_b) = \left( \frac{\sum_{ij} I_{ij} x_{ij}}{\sum_{ij} I_{ij}}, \frac{\sum_{ij} I_{ij} y_{ij}}{\sum_{ij} I_{ij}} \right) \tag{3}$$

Where $x_{ij}$ and $y_{ij}$ are the x and y co-ordinate components of each pixel, $I_{ij}$ is the intensity value at each pixel and $\sum_{ij}$ is the summation pixel-wise. As can be seen in equation 3 the centroiding method is fairly trivial, the part that determines the computational operations needed is the i and j terms. These terms are the 'window' of pixels that have been chosen by another rough estimator to get a generalised position, the window is a square around the estimated position so the computation scales like $n^2$, where n is the window size or box size.[11]

## B. Fitting methods

### 1. Point Spread Function

Point Spread Functions(PSF) is the way an object blurs due to the imaging of a point source of light, it is the reason the diffraction limit of a microscope is 250nm (in the x,y direction) and $>$450-700nm (in the z direction).[2] The PSF is also the smallest resolvable detail that can be seen with light as other objects that emit light that are smaller than one another all appear to be the same size. Provided that laboratory equipment is set up correctly, i.e. the lens is corrected for aberrations and constants are known such as aperture and angels between lens and samples, methods like the Richards-Wolf model and Gibson-Lanni model will calculate the centre of a spot near perfectly. The problem with these methods is that they are complicated and slow, and also offer an answer that is unnecessarily accurate for most applications. [12][13]

### 2. Gaussian

Where the exact prediction of section (II B 1) fails Gaussian fitting tries to succeed by presuming that, if all equipment is set up correctly, the centre of a PSF of a point source is always going to be in the centre. Thus for 2-D spot finding that can't afford the computational time of the previous method uses the more simple equation:

$$I(x, y) = I_0 \cdot \exp\Big(-a \cdot k^2((x - x_0)^2 + (y - y_0)^2)\Big) + b \tag{4}$$

Where k is $\frac{2\pi}{\lambda}$, $a$ is the width of the PSF, $I_0$ is the peak intensity and b is the average background per pixel. [13] A Gaussian fit is going to mostly cover the shape of a point source of light, especially

since the airy disk rings on the periphery of the center of the function do not determine the where the center is.

The Gaussian method usually uses one of two fitting methods, least-squares criterion (LS) or the maximum-likelihood estimation (MLE). [13] LS equation is as follows:

$$S = \sum_{pixels} \frac{(data - model\ prediction)^2}{expected\ variance\ of\ data} \tag{5}$$

The error (S) in the LS model is the subtracted difference between the predicted signal and the actual data itself squared, over the expected variance. The expected variance is the variation of the signal of that pixel, meaning if a bad error (S) is obtained that does not necessarily mean a bad prediction was given. Parameters in the Gaussian are altered and the error (S) is minimised to an acceptable amount and thus a fit is then obtained.

MLE is more complicated and is based on the idea that there is, like the name suggests, a maximum limit for the achievable accuracy. This is due to variance in noise, this is why MLE requires a model of the PSF and all forms of noise that the camera has.

### *3. Triangular method*

The triangle method being used takes inspiration from the Gaussian method, in which, a Gaussian curve is produced and the area is calculated by integrating the function. After this the position of the spot is estimated by a hyper-parameter optimisation method which minimises the residual area left over from the fitting process. This triangle method looks to reduce the computational load by removing the integration step, this can be done as the area of a triangle is just $\frac{1}{2}\ base \cdot height$. On top of this, the method also sums pixel intensities across axis, firstly it gives a better signal to noise ratio but also it means the triangle only needs to be rendered in 2 dimensions instead of 3, further reducing the computational time. Analogous to equation 4, the triangle method function takes three parameters; center, half base and height, from this the three points of a triangle are calculated. The residual seen in figure 2 is calculated similarly to equation 5 the image data is subtracted from a prediction, then the difference is squared and summed pixel-wise.

$$Residual = \sum_{pixels} (spot\ data - model\ prediction)^2 \tag{6}$$

The optimisation of this method uses a simple grid search to try and find the minimum of equation 6.

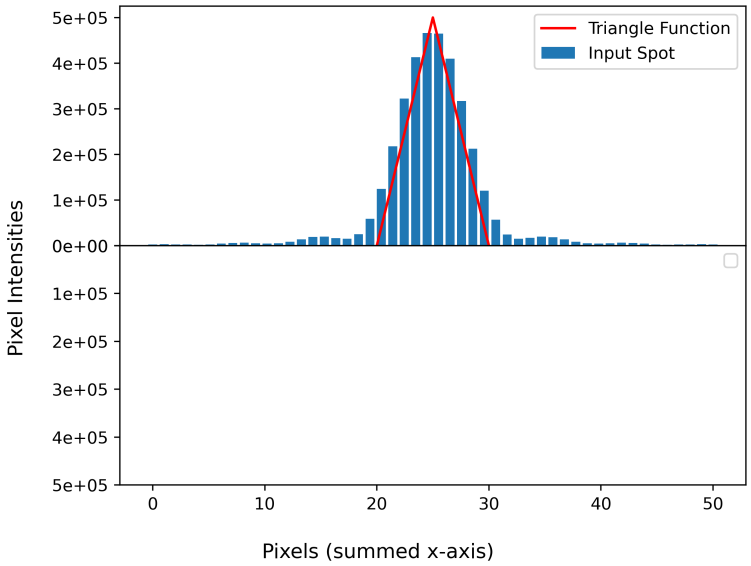


Figure 1. Graph of ideal spot data

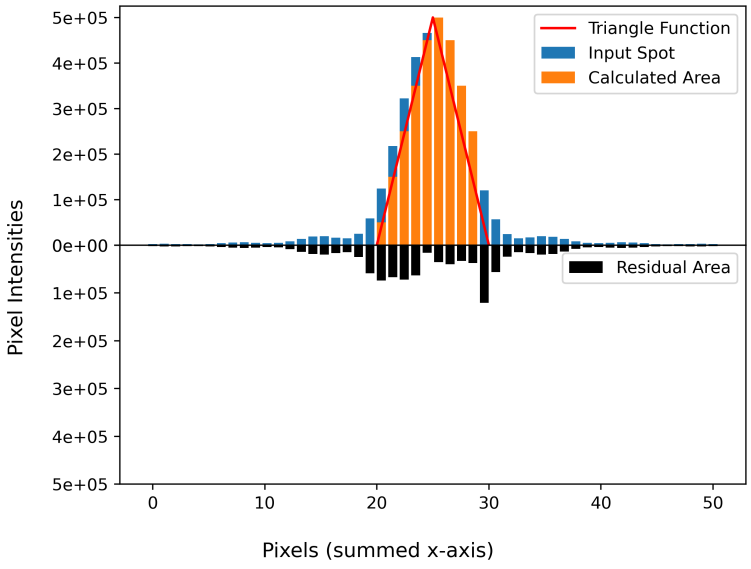


Figure 2. Graph of data from figure 1 with the calculated area and residual

As can be seen in figure 2 the area of the simulated spot are subtracted from the area under the triangle and a residual is left over, this residual parameter is the variable to be minimised for in the optimisation routine.

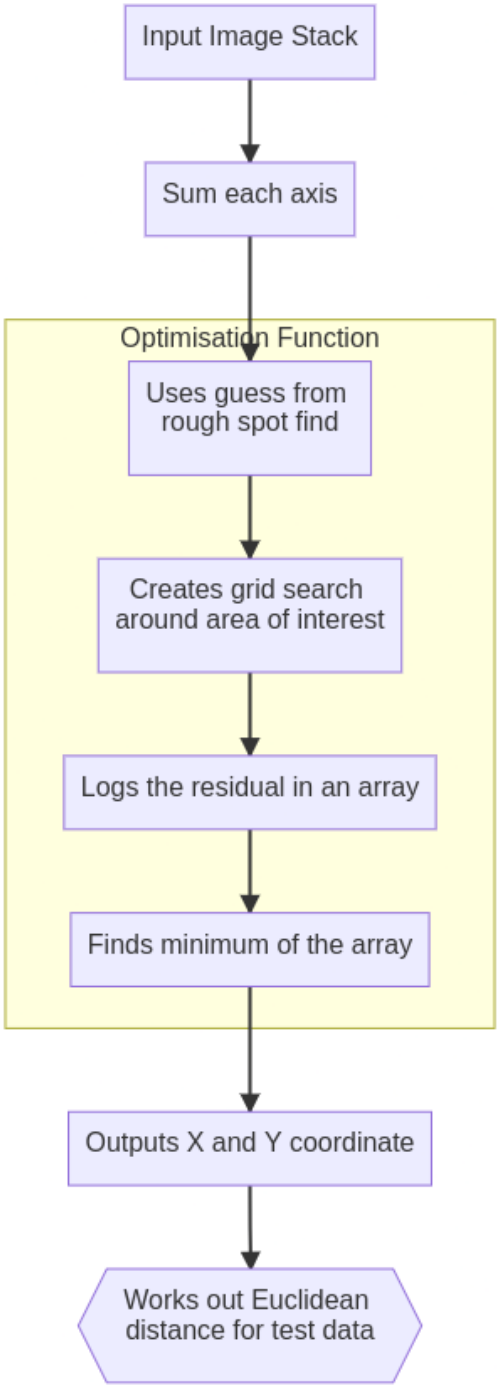


Figure 3. Flowchart describing how the code for the triangular fitting method works

Once the triangle algorithm was implemented it was tested on TIFF stacks of 100 images of perfect spot data. The absolute error (Euclidean distance) was calculated from each axis and plotted as seen in figure 4 A. In image B a histogram was produced so that the spread was more visible.

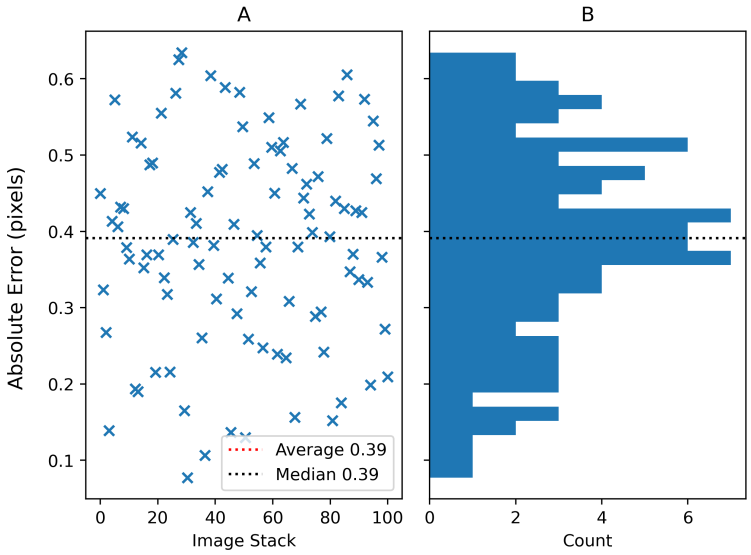


Figure 4. A: Absolute error from the ground-truth for R1.00, B: A histogram of errors from graph A

# III. Results and analysis

## A. Centroiding

For the centroiding method box sizes of 3, 5, 7 and 11 were used in the production of the histograms pertaining to the absolute error, this was done for the noisy data as well. The rest of the data not presented in the main body of text is available in the appendix section (A). In all figures for centroiding, all of the combined histograms had taken $\approx 1.4 \cdot 10^{-4}$ seconds for all radii and all 100 images in the TIFF stack. This means per spot the time taken to calculate and answer was $\approx 2 \cdot 10^{-7}$ seconds

The results of the centroiding algorithm in figure 5 show a fairly poor level of accuracy, ranging from a $0 \rightarrow 1.5$ pixel error approximately. This lack of accuracy is especially pronounced the larger the radii of spot, the reason for this increasing error is due to the spots being larger in the same sized 50x50 images. The radii of the airy disk that was used to generate the spots is 'physically' larger than the box size that the centroiding is using. This holds true for the radii that are larger than R1.5 as the box size's diameter, as well as the diameter of the airy disk, is 3 pixels. The further increase of inaccuracy seen in figure 5 R4.00, R5.66 and R8.00 is due to the 3x3 box being placed roughly where the centre of the spot already is, then the algorithm is ran which in essence takes the average of the intensities. This 3x3 box is not given a reasonable range of intensities to average over thus the method will be less likely to give the correct answer, this instead gives a range of answers from $0 \rightarrow 1.5$ pixels approximately as if the local maximum finder roughly gives an answer the centroiding algorithm will only give and answer that is 1.5 pixels off of that guess. Since in this perfect data that only has one spot per image, the local maximum finder will predict where the spot is to a single pixel of accuracy thus the maximum error seen should indeed be fractionally larger than 1.5 pixels as observed.

In figure 6 noisy spot data was provided to test out the algorithms on, these spot were the same as before but with read noise at 1 electron, average photon number per spot at 2000 and dark current at 0.1 electron per pixel and cg? Also the number of radii were reduced, R1.00 and R1.41 were removed. These noise values were chosen to replicate real world noise levels in order to test all algorithms in isolation from any other variables so that the spot finding methods could be objectively

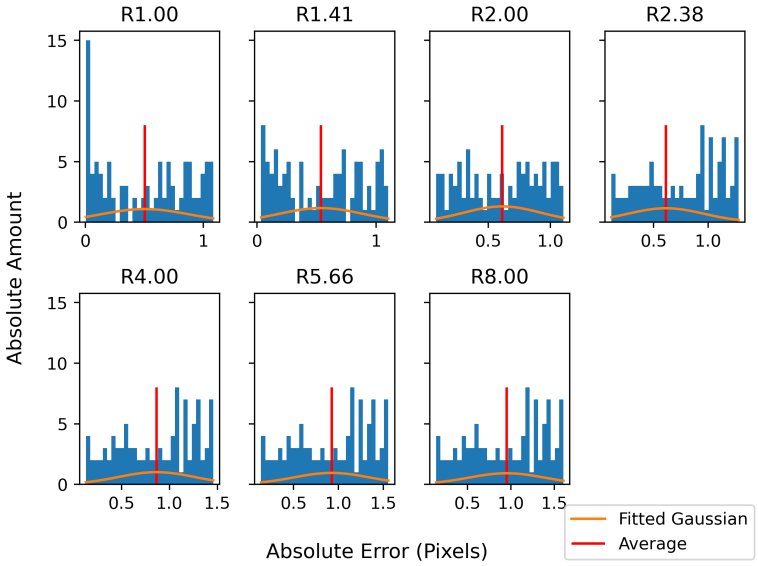


Figure 5. Histograms of the absolute error from each radii with a box size of 3x3 pixels. Completed in $\approx 1.4 \cdot 10^{-4}$s

observed.

The noisy data for the 3x3 centroid box size did not have a pronounced impact on average accuracy per radii. This again is due to the size of the box being small relative to the size of the spots, thus mostly not allowing the noise to play a part in the calculation of the centre of the spot. One difference that the noisy data does seem to show is that it gives a more even spread of answers around it's average, this suggests that although the noisy data is not changing the average it is having an effect on the centroiding algorithm. The limiting factor in this case is the box size in which the algorithm is interested in.

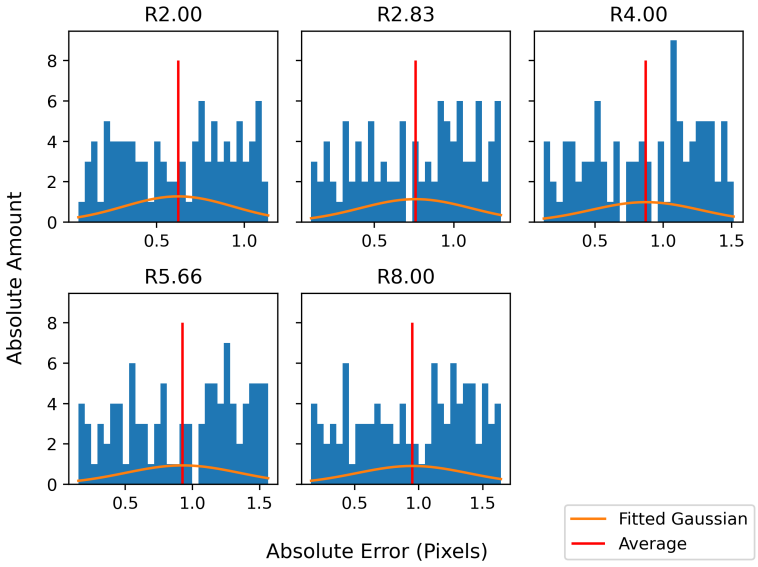


Figure 6. Histograms of the absolute error from each radii with a box size of 3x3 pixels, with noise.

In figure 7 the box size used was 11x11, this increases the sub-pixel localisation drastically compared to figure 5. The spread of all answers is smaller using 11x11 instead of using 3x3 boxes,

the spread also changes with radii sequentially getting larger along with the average. This is due to the larger box size being able to fit more pixels in to average over effectively, this is clearly evident in the R5.66 and R8.00 histogram as there is a significant jump in inaccuracy as the radii is still larger than the radii of the box.

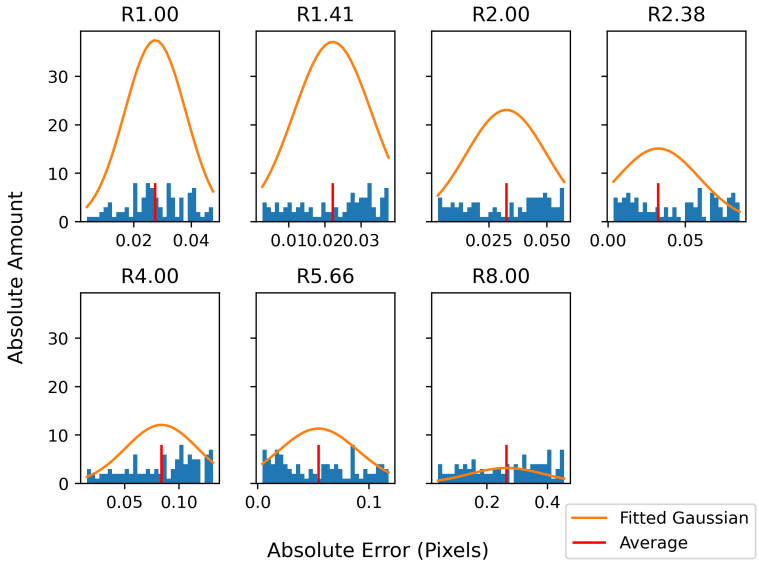


Figure 7. Histograms of the absolute error from each radii with a box size of 11x11 pixels.

In figure 8 when centroiding was used on the noisy data with an 11x11 box size, on average the accuracy decreased as expected and gave a similar average error for each radii apart from R8.00. Again this will be due to the fact that the R8.00 spot will not fit into the box size being calculated but also in relation to the spot, as the size of the spot increases so to does the noise in the images provided.

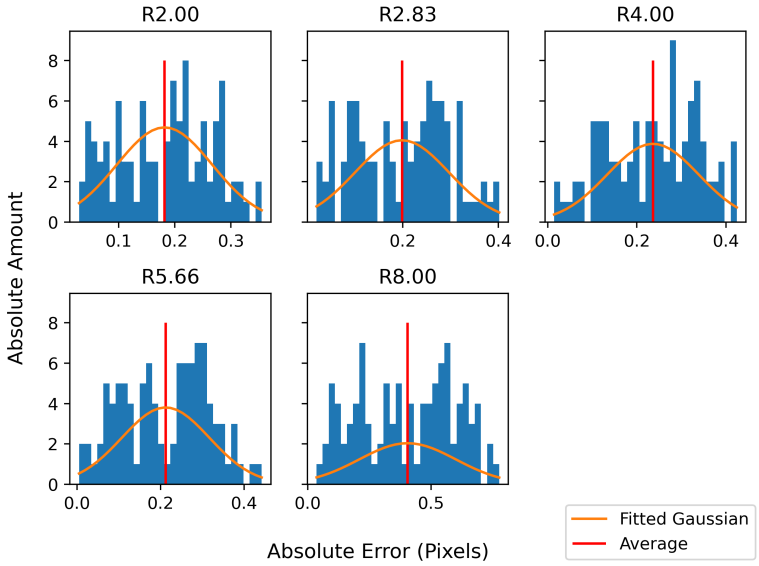


Figure 8. Histograms of the absolute error from each radii with a box size of 11x11 pixels, with noise.

In figure 9 the box size for making the centroiding calculation was varied from 3 to 15 pixels$^2$ in odd increments, this was tested to understand the relationship between box size and accuracy. In

general the larger the box size the more accuracy gained this was expected especially for the perfect data as there was only one spot per image, although this would be impractical for real data as spot are more than likely to be closer than $\approx 15$ pixels.

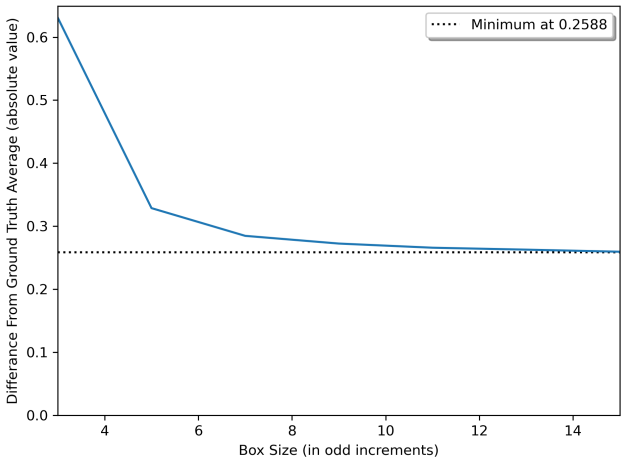


Figure 9. Showing the accuracy of centroiding Vs the box size chosen, for a radii or R2.00.

Figure 10, similar to figure 9, shows the accuracy of the centroid method against the varying box size, but on a set of noisy data. Here it can be seen that for a period of box size increases the accuracy also increases, then it minimises and then decreases indefinitely. This specific box size minimises the error at $\approx 9$ pixels due to the radii being R2.00, as each spot size will be optimised at a certain box size that's more than double it's radii. For noisy spots this optimisation can not be too large as the centroiding algorithm is known for being highly sensitive. [10]

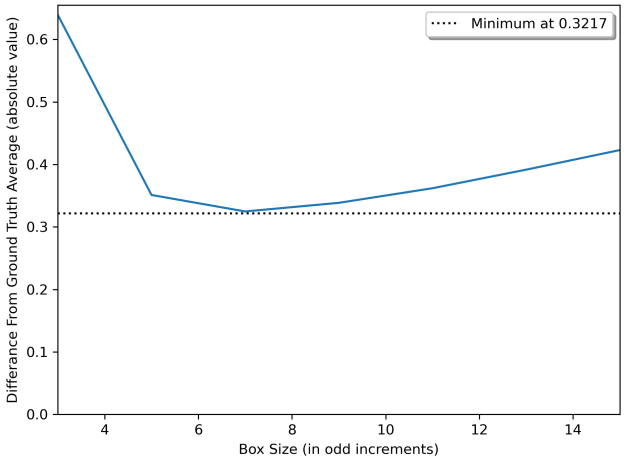


Figure 10. Showing the accuracy of centroiding Vs the box size chosen, for a radii or R2.00 and with noise

## B. Triangle Fitting

In figure 17 it can be seen that while using simulated data of radii R1.00, the mean accuracy of the localisation is $\approx 0.4$ of a pixel whilst being executed in $\approx 0.34$ seconds. This time to complete a computation was the same for all individual radii, for all the data the time taken was $\approx 2.4$ seconds.

This means an average time to calculate a spot using the triangle method takes $\approx 3.3 \cdot 10^{-3}$ seconds.Part C of figure 17 has been replicated for all simulated spots given in figure 18 to compare how the change in spot size changes accuracy. Figure 11 shows the histogram results of the triangle fitting method on the perfect simulated data. Compared with the 3x3 centroiding method (figure 5) the average accuracy of this method is better, especially for the larger radii, ranging from a $\approx 1.33 \rightarrow 2.6$ times improvement. This comes at a $\approx 16500$ times increase in computational time to produce an answer however. A reason for this apparent increase in accuracy will be because of the fact that the box size is limiting the amount of the image the centroiding method can calculate over. If this method is compared with the 11x11 centroiding method (figure 7) then there is a substantial difference in average accuracy, ranging from $\approx 19 \rightarrow 1.25$ times better accuracy for the centroiding method whilst also still having a $\approx 16500$ times computational speed advantage.

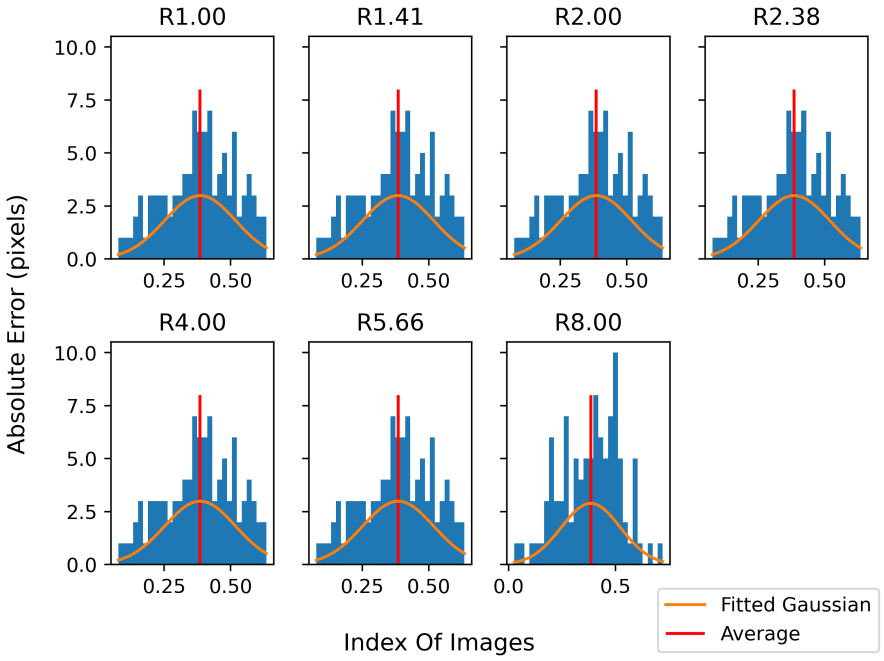


Figure 11. Histograms of the absolute error from each radii

As can be seen in figure 12, compared with figure 11, the distribution of results is shifted towards being less accurate. This is expected as noise adds randomness and variability into the system, giving extra information that does not aid in the process of finding the centre of a spot. If figure 12 is compared with figure 8, again, it can be seen that the centroiding method achieves better results, ranging from $\approx 1.5 \rightarrow 2$ times more accurate than the triangle method and again being $\approx 16500$ times faster.

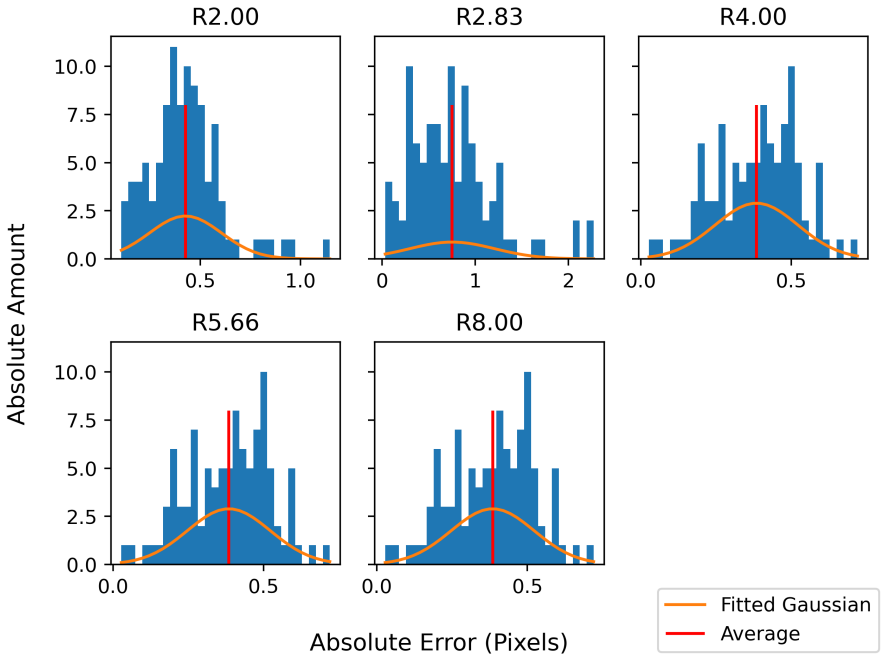


Figure 12. Histograms of the absolute error from each radii, but with noise

# IV. Discussion

In a paper by delabie et al. [10] known algorithms for spot finding were compiled and tested for accuracy and efficiency, this includes variations of the centroid and Gaussian fit methods. The method used for centroiding that was used to test against the triangle method in this paper was attained from delabie et al. [10] and was referred to as the centre of gravity method. In which when it was tested it was found to take in the range of $0.055 \rightarrow 0.253 \cdot 10^{-6}$ seconds to calculate the position of one star. This is in contrast with the time taken to calculate a single spot in this paper which took $\approx 2 \cdot 10^{-7}$ seconds, that's a $\approx 3.6 \rightarrow 1$ times increase to a in elapsed time. Comparing figure 9 with figure 4 in the delabie et al. [10], star tracker data was used from the Plato mission which had had very little noise and gave very accurate estimates. In comparison with figure 9, delabie et al. results had the same overall trend of gaining in accuracy as box size increased, however the results that figure 9 generated were larger in error. At it's minimum error the centroiding algorithm employed here gave a result of $\approx 0.26$, while the minimum error in the delabie et al. paper gave a result of $\approx 0.012$. Now comparing figure 10 with figures 2 & 3 in delabie et al. [10], again it can be seen that the general trend of the plots follows what was recreated here. In figure 10 the minimum error achieved is $\approx 0.32$ with a box size of 7, in delabie et al. the minimum errors in figure 2 & 3 are both $\approx 0.1$ whilst using a box size of 7. A reason for the discrepancy in both results may be due to the data used, as for the centroiding methods, accuracy seems to be dependant the spot size in relation to the box size. The elapsed time difference between the centroiding method and the triangle method were to be expected from the outset, as the centroiding method has been used for star tracking from $1975 \rightarrow 1978$ and only relies on two multiplications, two divisions and four summations to provide an answer. Centroiding is also considered to be the fastest spot finding method.[10]

A reason for the centroiding method and triangle method used in this paper being slower that others may be due to the fact that the code for this paper was written in python, where as the centroiding method used in delabie et al. was written in C++. Elapsed time test results taken

from a website that poses the question Which programming language is the fastest?[14], range from $\approx 2.5 \rightarrow 95$ times less time taken for C++ over python. This is however dependant on what is being ran, for example the largest gap in elapsed time was from a symplectic-integrator that modeled planets and the smallest gap was from a program that takes in strings of amino acid protein sequences and formats them. This means that what specific operations are carried out on either language play a role in how fast the program runs, in part due to the fact that python is an interpreted language whilst C++ is a compiled language. Another reason for this papers shortfall in computational time taken may be due to the use of python packages used, this includes pandas, matplotlib, scipy, tifffile and others need to be called from a different file. An improvement could be defining the functions that are used in the same file they are being used in.

A potential reason for the lack of accuracy in the method created could be attributed to the fact that this method is a worse approximation of a spot than a Gaussian or an airy function. While these other methods map more closely to a PSF, of which a diffraction limited point source of light follows, the triangle method either over or under laps the shape of the spot (seen in figure 1 & 2) possibly making a fitting function produce the errors observed.

## A. Future work

A possible fix for the current lack in accuracy with the triangle method could be modifying the triangle function in a way that geometrically adds more area. This is to say that the shape of the function should no longer just be a triangle but should also cover more area in a way that better fits an PSF. This may fix the current accuracy issues as the under and overlap of area that a PSF and a triangle have, may happen in such a way that disrupts the fitting function. The benefit that this would still retain over a method like the Gaussian fitting one would be the area calculation, whilst being more complex, would still be less computationally intensive than an integration.

Another idea that could potentially be worthwhile to investigate for spot finding could be using the pre-existing method that works, for example Gaussian fitting, but trying to simplify it or approximate it. This could mean producing a look up table of pre-calculated Gaussian functions that could be fitted to a spot. This would in theory produce, provided a large enough look up table, a guess for the center of a spot with a similar accuracy to a normally fitted and integrated function, whilst also having a elapsed time advantage.

# V. Conclusion

To conclude a spot finding method was created and others were replicated in order to compare accuracy and time taken. In section I important concepts about sub-pixel localisation were discussed to give an overarching view what it is and why this paper was trying to improve it in some manner. In section II the procedures that were carried out like centroiding and the Gaussian fitting method were explained step by step to understand the apparent costs and benefits of well understood and common place algorithms. Furthermore a new method was created and discussed in order to align with the motivation behind the study of trying to produce a method that is still fast in terms of time taken to give an answer but also more accurate than an algorithm like centroiding. In section III the centroiding and triangle algorithms were tested with spot data provided, for the simulated perfect data this resulted in the centroiding algorithm predictably being faster (16500 times) and being more accurate ($\approx 19 \rightarrow 1.25$ times) except from the case of the 3x3 box size where the triangle method has better accuracy ($\approx 1.33 \rightarrow 2.6$ times). In the case of the simulated noisy data, again, the centroiding method takes the advantage with results more accurate ($\approx 1.5 \rightarrow 2$ times). Additionally in section IV we discussed potential reasons on why the method created and other methods used perform worse than methods executed in cited papers. Following this critique

in section IV A improvements were discussed that will be investigated further in future work to be conducted. Overall, even though the method created failed to produce better results than initially hoped, it still shows promise and demands further study. During the process of this paper I have greatly expanded my knowledge of microscopy, fluorescence, computing and in general how to develop methods to try and solve problems.

# References


[1] Mats GL Gustafsson. Surpassing the lateral resolution limit by a factor of two using structured illumination microscopy. *Journal of microscopy*, 198(2):82–87, 2000.

[2] Catherine G Galbraith and James A Galbraith. Super-resolution microscopy at a glance. *Journal of cell science*, 124(10):1607–1611, 2011.

[3] Sebastian van de Linde, Steve Wolter, and Markus Sauer. Single-molecule photoswitching and localization1. *Australian Journal of Chemistry*, 64(5):503–511, 2011.

[4] Claude Elwood Shannon. Communication in the presence of noise. *Proceedings of the IRE*, 37(1):10–21, 1949.

[5] R.F. Graf. *Modern Dictionary of Electronics*. Newnes, 1997.

[6] Graham T. Dempsey. Chapter 24 - a user's guide to localization-based super-resolution fluorescence imaging. In Greenfield Sluder and David E. Wolf, editors, *Digital Microscopy*, volume 114 of *Methods in Cell Biology*, pages 561–592. Academic Press, 2013.

[7] Philip Tinnefeld, Christian Eggeling, and Stefan W Hell. *Far-field optical nanoscopy*, volume 14. Springer, 2015.

[8] Juan Castorena and Charles D. Creusere. Sub-spot localization for spatial super-resolved lidar. In *2013 IEEE International Conference on Acoustics, Speech and Signal Processing*, pages 2227–2231, 2013.

[9] Nico Calitz. *The design and implementation of a stellar gyroscope for accurate angular rate estimation on CubeSats*. PhD thesis, Stellenbosch: Stellenbosch University, 2015.

[10] Tjorven Delabie, Joris De Schutter, and Bart Vandenbussche. An accurate and efficient gaussian fit centroiding algorithm for star trackers. *The Journal of the Astronautical Sciences*, 61(1):60–84, 2014.

[11] Ronald C Stone. A comparison of digital centering algorithms. *The Astronomical Journal*, 97:1227–1237, 1989.

[12] Bernard Richards and Emil Wolf. Electromagnetic diffraction in optical systems, ii. structure of the image field in an aplanatic system. *Proceedings of the Royal Society of London. Series A. Mathematical and Physical Sciences*, 253(1274):358–379, 1959.

[13] Alex Small and Shane Stahlheber. Fluorophore localization algorithms for super-resolution microscopy. *Nature methods*, 11(3):267–279, 2014.

[14] Doug Bagley. Which programming language is fastest?, 2001. https://benchmarksgame-team.pages.debian.net/benchmarksgame/index.html.

# A. Appendix

All code developed or used for this project is available on GitHub along with the spot data generated. `https://github.com/AntonGashi/4th_year_project`

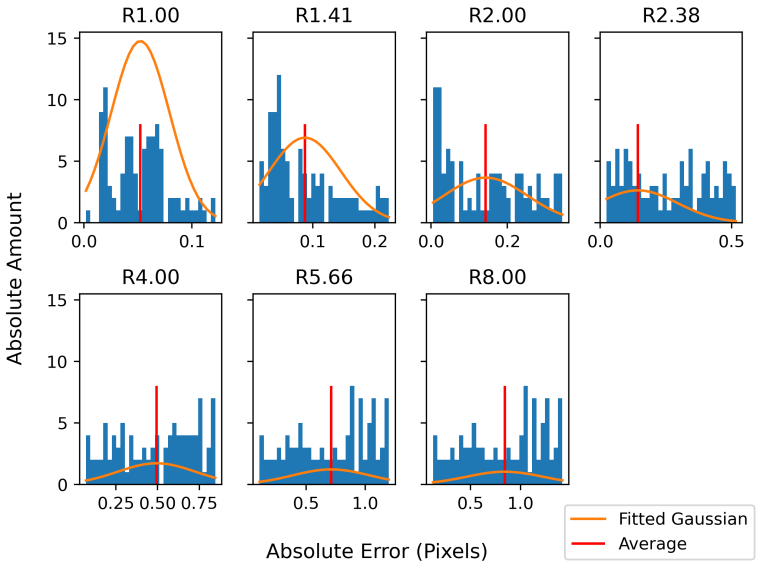


Figure 13. Histograms of the absolute error from each radii with a box size of 5x5 pixels.

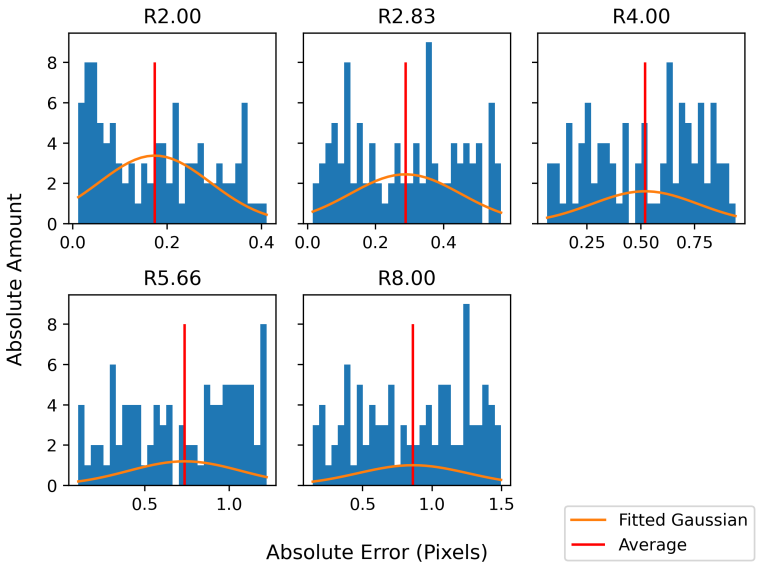


Figure 14. Histograms of the absolute error from each radii with a box size of 5x5 pixels, with noise.

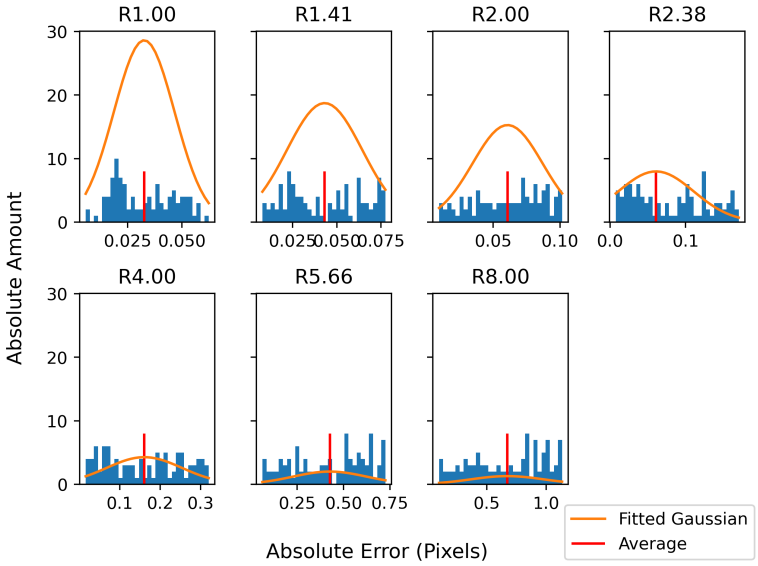


Figure 15. Histograms of the absolute error from each radii with a box size of 7x7 pixels.

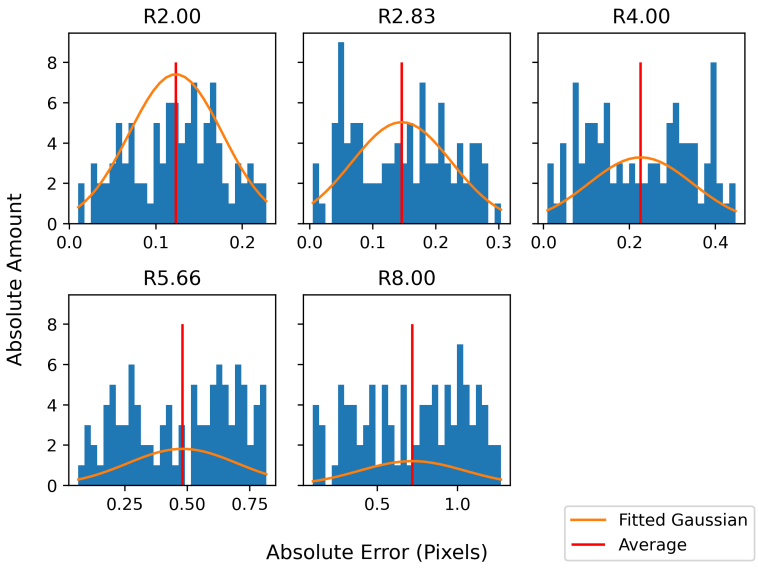


Figure 16. Histograms of the absolute error from each radii with a box size of 7x7 pixels, with noise.

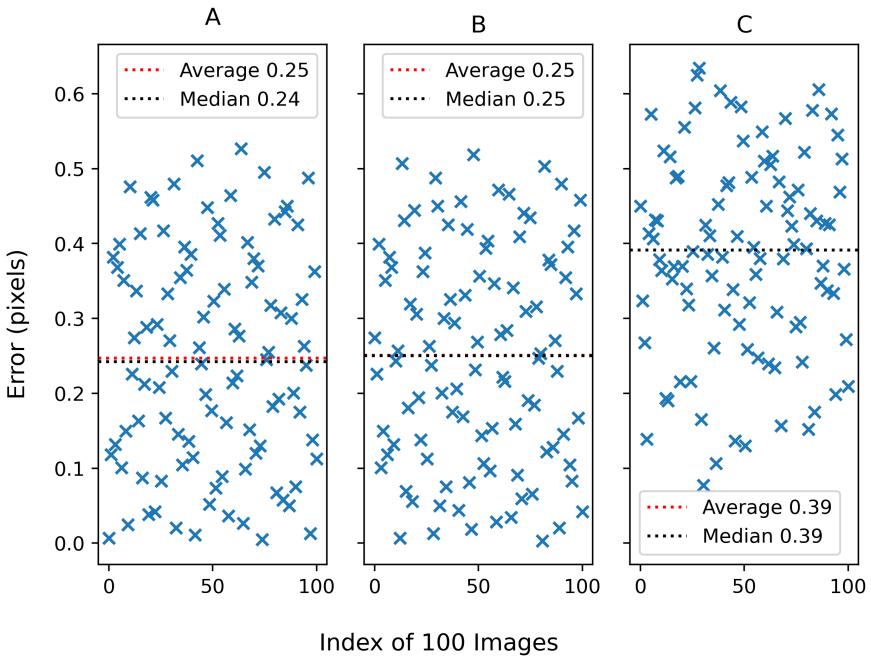


Figure 17. Simulated spots with R1.00, A: Error in the X direction, B: Error in the Y direction, C: Absolute error from the ground-truth

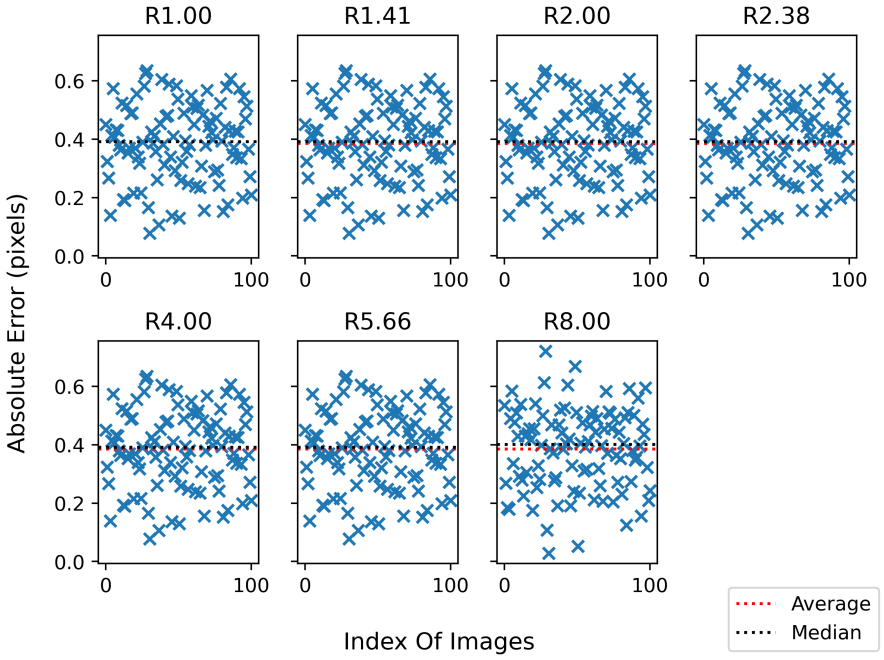


Figure 18. Spot localisation (like graph C in figure 17) of different radii, R, on perfect data (executed in 2.4s)

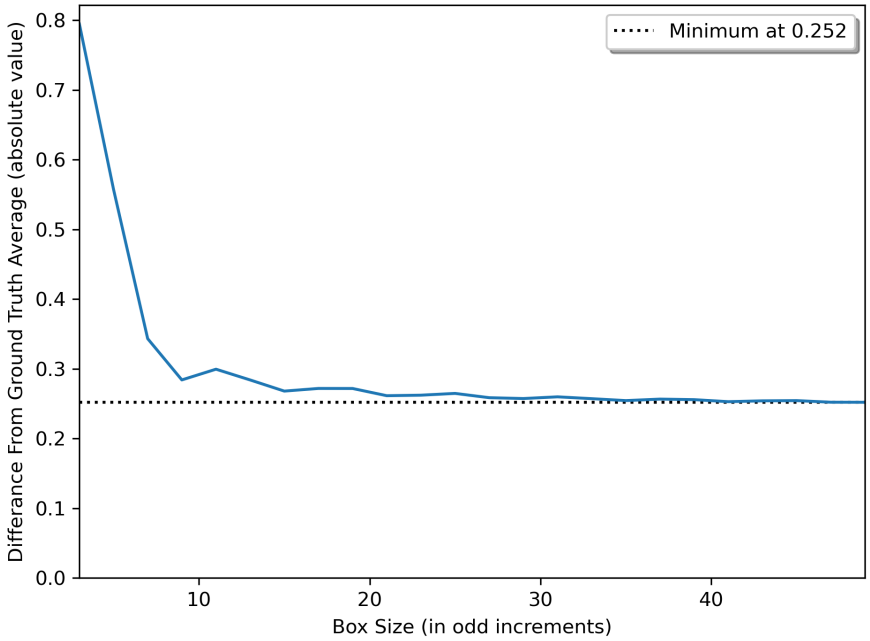


Figure 19. Showing the accuracy of centroiding Vs the box size chosen (from 3 to 49), for a radii or R4.00 and without noise

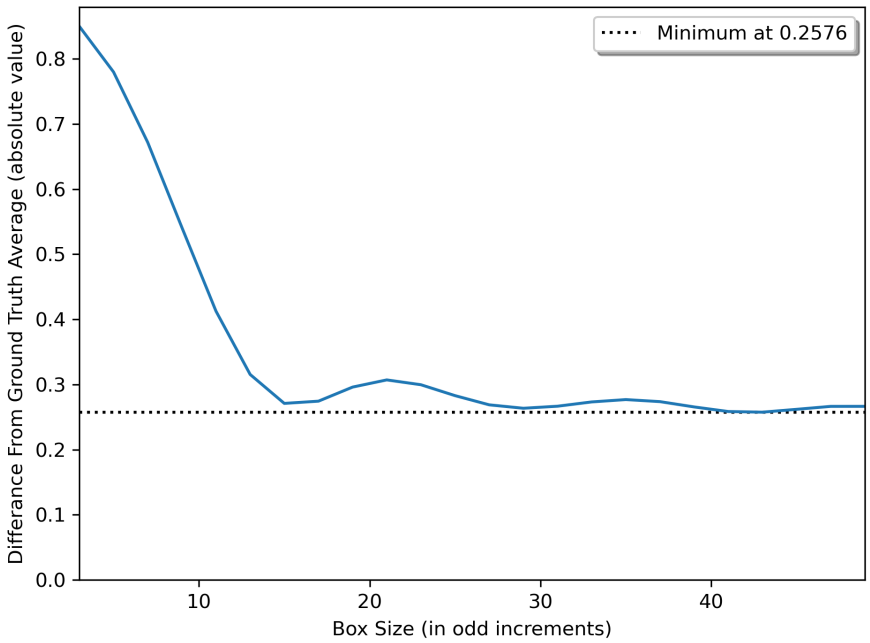


Figure 20. Showing the accuracy of centroiding Vs the box size chosen (from 3 to 49), for a radii or R8.00 and without noise

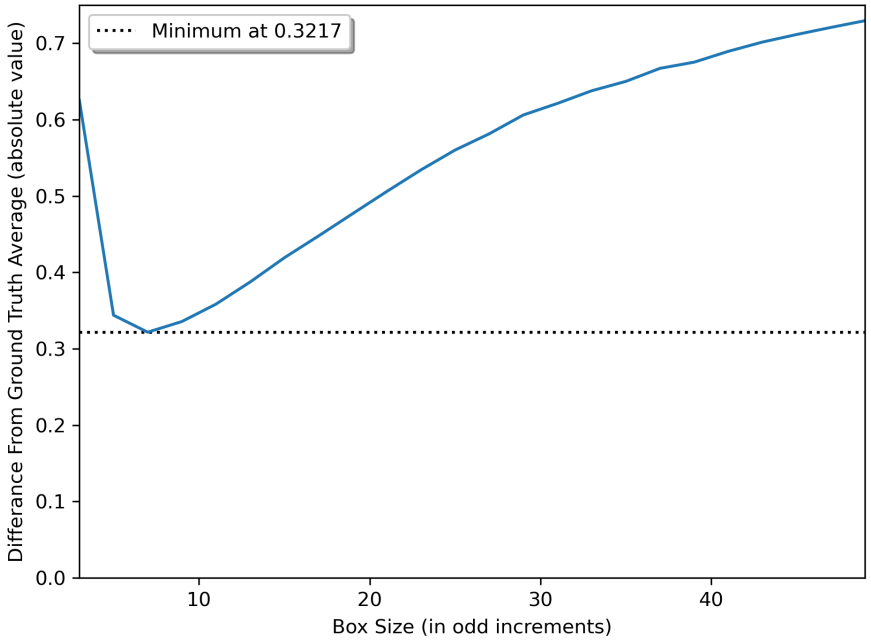


Figure 21. Showing the accuracy of centroiding Vs the box size chosen (from 3 to 49), for a radii or R2.00 and with noise

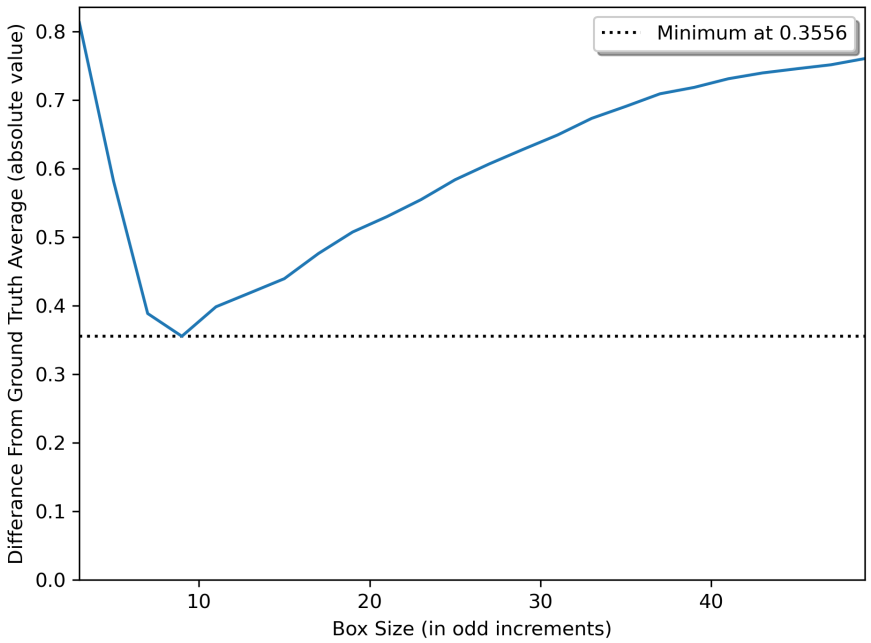


Figure 22. Showing the accuracy of centroiding Vs the box size chosen (from 3 to 49), for a radii or R4.00 and with noise

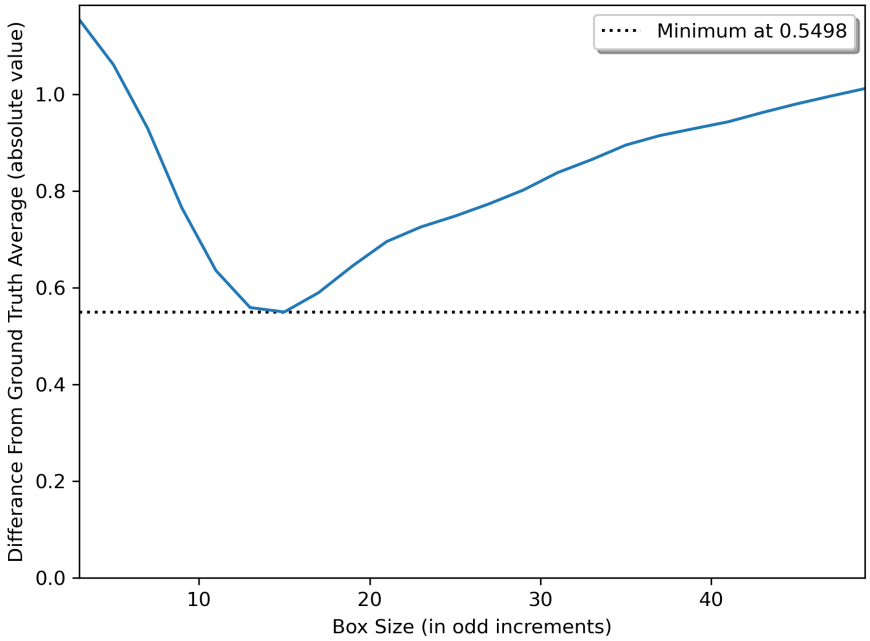


Figure 23. Showing the accuracy of centroiding Vs the box size chosen (from 3 to 49), for a radii or R8.00 and with noise